

Driven-Dissipative Rydberg Blockade in Optical Lattices

Javad Kazemi^{✉*}

Institut für Theoretische Physik, Leibniz Universität Hannover, Appelstraße 2, 30167 Hannover, Germany

Hendrik Weimer[†]

*Institut für Theoretische Physik, Leibniz Universität Hannover, Appelstraße 2, 30167 Hannover, Germany
and Institut für Theoretische Physik, Technische Universität Berlin, Hardenbergstraße 36 EW 7-1, 10623 Berlin, Germany*

 (Received 30 August 2022; revised 18 March 2023; accepted 3 April 2023; published 19 April 2023)

While dissipative Rydberg gases exhibit unique possibilities to tune dissipation and interaction properties, very little is known about the quantum many-body physics of such long-range interacting open quantum systems. We theoretically analyze the steady state of a van der Waals interacting Rydberg gas in an optical lattice based on a variational treatment that also includes long-range correlations necessary to describe the physics of the Rydberg blockade, i.e., the inhibition of neighboring Rydberg excitations by strong interactions. In contrast to the ground state phase diagram, we find that the steady state undergoes a single first order phase transition from a blockaded Rydberg gas to a facilitation phase where the blockade is lifted. The first order line terminates in a critical point when including sufficiently strong dephasing, enabling a highly promising route to study dissipative criticality in these systems. In some regimes, we also find good quantitative agreement of the phase boundaries with previously employed short-range models, however, with the actual steady states exhibiting strikingly different behavior.

DOI: [10.1103/PhysRevLett.130.163601](https://doi.org/10.1103/PhysRevLett.130.163601)

Strongly interacting Rydberg atoms undergoing driving and dissipation allow the study of a wide range of many-body effects not seen in their equilibrium counterparts, ranging from dissipative quantum sensors [1] to self-organizing dynamics [2]. These effects are enabled by the presence of a strong van der Waals interaction between the atoms, which is fundamentally long ranged. Yet, very little is known about the many-body properties of such systems, as long-ranged open quantum systems are inherently hard to simulate on classical computers [3]. Here, we present a variational calculation of the steady state phase diagram of a long-range interacting Rydberg in an optical lattice.

A key feature of strongly interacting Rydberg gases is the appearance of the Rydberg blockade, where the strong van der Waals interactions prevent the excitation of neighboring Rydberg atoms [4–9]. However, given the intrinsic challenges associated with the treatment of open quantum many-body systems, most works studying dissipative Rydberg gases have employed short-range interactions [10–16], which are inadequate for strongly blockaded Rydberg gases. As a consequence, the steady state phase diagram of blockaded Rydberg gases is essentially unknown.

In this Letter, we present the application of a variational approach for the nonequilibrium steady state of Rydberg atoms with strong repulsive van der Waals interactions. Notably, we explicitly account for correlations between multiple Rydberg excitations. Based upon the variational results, we find a dissipative variant of the Rydberg

blockade in the pair correlation function, where any simultaneous excitation within a certain blockade radius is strongly suppressed. In addition, we investigate the interplay between coherent driving and dissipation, finding a first-order dissipative phase transition, which terminates in a critical point under sufficiently strong additional dephasing. Finally, we analyze the validity of effective short-range models to describe the dynamics even in the blockaded regime, where we find that such effective models actually perform better in the presence of a strong Rydberg blockade when it comes to the computation of phase boundaries; however, the properties of the steady states significantly differ between the long-range and short-range models.

Model.—Dissipative processes involving electronic excitations can often be described in terms of a Markovian master equation in Lindblad form as the frequency of the emitted photons provides for a natural separation of time-scales required for the Markov approximation [17]. Then, the time evolution of the density matrix ρ is given by

$$\mathcal{L}(\rho) = -i[H, \rho] + \sum_{j=1}^N \sum_{k=1}^M \left[c_j^{(k)} \rho c_j^{(k)\dagger} - \frac{1}{2} \{c_j^{(k)\dagger} c_j^{(k)}, \rho\} \right], \quad (1)$$

where \mathcal{L} denotes the Liouvillian superoperator $\mathcal{L}(\rho) = \partial_t \rho$, which consists of a coherent part represented by the Hamiltonian H and a dissipative part characterized a set

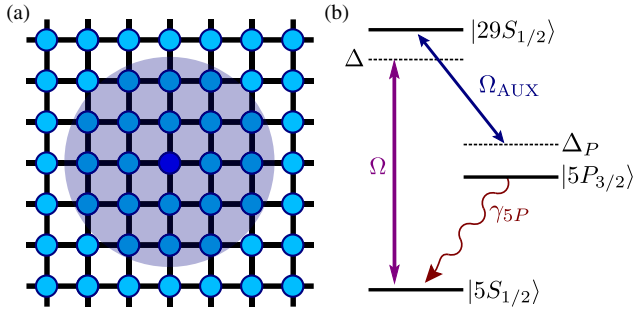


FIG. 1. Setup of the system. (a) Strong van der Waals repulsion leads to a blockade of simultaneous Rydberg excitations over a number of sites of the square lattice. (b) Internal level structure showing a two-photon excitation of a single Rydberg state with a Rabi frequency Ω and a detuning Δ , as well as laser-assisted dissipation via an intermediate excited state.

of jump operators $c_j^{(k)}$ with $j(k)$ running over N constituents (M dissipation channels). The coherent dynamics of a ground state atom being laser driven to a single Rydberg state can be expressed in a spin 1/2 Hamiltonian as

$$H = -\frac{\hbar\Delta}{2} \sum_{i=1}^N \sigma_z^{(i)} + \frac{\hbar\Omega}{2} \sum_{i=1}^N \sigma_x^{(i)} + C_6 \sum_{i<j} \frac{P_r^{(i)} P_r^{(j)}}{r_{ij}^6}, \quad (2)$$

where Ω is the driving strength, Δ is the detuning from the atomic resonance, and C_6 denotes the strength of the repulsive van der Waals interaction [18,19] involving the projector $P_r^{(i)}$ onto the Rydberg state. In our work, we consider the atoms being loaded in a two-dimensional optical lattice, see Fig. 1. The derivation of the jump operators c_j is more subtle [20], but laser-assisted dissipation via an intermediate electronic excitation allows the use of effective jump operators of the form $c_j^{(1)} = \sqrt{\gamma} \sigma_-^{(j)}$, with γ being the effective decay rate from the Rydberg state into the ground state [21]. Furthermore, this setup has the advantage that it allows tuning of the dissipation rate independently from the other properties of the Rydberg state such as the C_6 coefficient. Here, we also assume that the laser-mediated decay is much faster than the natural decay of the Rydberg excitation or changes in the Rydberg state by blackbody radiation, therefore we neglect these processes. In addition to the dissipation, we also allow for a second set of jump operators $c_j^{(2)} = \sqrt{\gamma_p} \sigma_z^{(j)}$, where γ_p denotes a dephasing rate arising, e.g., from noise of the driving laser.

Concerning the experimental setup, we consider a square optical lattice trapping Rubidium-87 atoms with a lattice spacing of $a = 532$ nm. Here, we consider laser driving from the electronic ground state by a two-photon transition to the state $|29S_{1/2}\rangle$, which has a van der Waals coefficient of $C_6 = h \times 17$ MHz μm^6 [32].

Variational treatment of long-range correlations.—In the following, we will be interested in the properties of the nonequilibrium steady state given by the condition $\partial_t \rho = 0$. Following the variational principle for steady states of open quantum systems [11], we turn to a variational parametrization that also allows for long-range correlations, which are crucial to capturing the physics of the Rydberg blockade. For the trial state, we consider a variational ansatz containing local density matrices as well as long-range two-body correlations in the following form:

$$\rho_{\text{var}} = \prod_{i=1}^N \rho_i + \sum_{i<j} \mathcal{R} C_{ij}, \quad (3)$$

where N is the number of sites, \mathcal{R} is a superoperator transforming the identity matrix \mathbb{I}_i into ρ_i , and $C_{ij} = \rho_{ij} - \rho_i \otimes \rho_j$ denotes the two-particle correlations. Crucially, we ignore higher-order correlations as in dissipative dynamics with power-law interactions they decay faster than two-body correlations [22]. The key properties of the variational ansatz are a parametrized algebraic correlation function for the Rydberg density, as well as exponentially decaying terms for the other correlation functions [21]. Considering the residual dynamics of the ansatz, we define a variational cost function that can be cast into the form

$$F_v \equiv N^{-1} \frac{\|\dot{\rho}_{\text{var}}\|_{\text{HS}}^2}{\|\rho_{\text{var}}\|_{\text{HS}}^2}, \quad (4)$$

where $\|O\|_{\text{HS}} = \sqrt{\text{Tr}[OO^\dagger]}$ is the Hilbert-Schmidt norm defined according to the inner product $\langle O, O' \rangle = \text{Tr}[OO'^\dagger]$. Using the definition of F_v for a translationally invariant system, and expanding the Liouvillian in terms of local and interacting terms, i.e., $\mathcal{L} = \sum_i \mathcal{L}_i + \sum_{i<j} \mathcal{L}_{ij}$, we end up with an efficiently computable upper bound, i.e., $F_v \leq f_v$, that reads as

$$\begin{aligned} f_v = & g_p^{-2} \sum_{1 \neq j} \langle \langle \rho_{\text{var}}^{(1j)} | \mathcal{L}_1^\dagger \mathcal{L}_1 + \mathcal{L}_1^\dagger \mathcal{L}_j | \rho_{\text{var}}^{(1j)} \rangle \rangle \\ & + g_p^{-3} \sum_{1 \neq j \neq k} \langle \langle \rho_{\text{var}}^{(1jk)} | 2\mathcal{L}_1^\dagger \mathcal{L}_{1j} + \mathcal{L}_1^\dagger \mathcal{L}_{jk} | \rho_{\text{var}}^{(1jk)} \rangle \rangle \\ & + g_p^{-4} \sum_{1 \neq j \neq k \neq l} \langle \langle \rho_{\text{var}}^{(1jkl)} | \frac{1}{2} \mathcal{L}_{1j}^\dagger \mathcal{L}_{1j} + \frac{1}{2} \mathcal{L}_{1j}^\dagger \mathcal{L}_{jk} \\ & + \frac{1}{2} \mathcal{L}_{1j}^\dagger \mathcal{L}_{1k} + \frac{1}{4} \mathcal{L}_{1j}^\dagger \mathcal{L}_{kl} | \rho_{\text{var}}^{(1jkl)} \rangle \rangle, \end{aligned} \quad (5)$$

where we used the notation $\|\dot{\rho}_{\text{var}}\|_{\text{HS}}^2 = \langle \langle \mathcal{L}^\dagger(\rho_{\text{var}}) | \mathcal{L}(\rho_{\text{var}}) \rangle \rangle$, and $g_p = \langle \langle \rho_1 | \rho_1 \rangle \rangle$ denotes the local purity [21].

Within this approach, we can also make statements about systems in the thermodynamic limit, even for finite N . This is possible, as within our variational approach, a system of N sites is indistinguishable from an infinitely large system

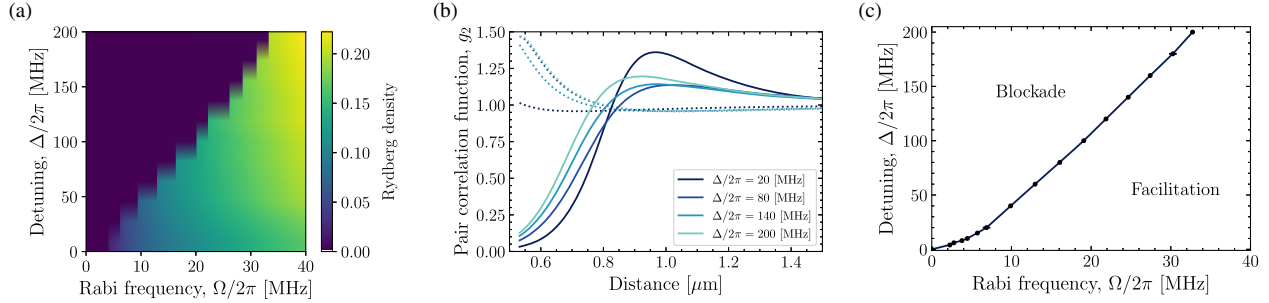


FIG. 2. Variational results for the steady state of two-dimensional driven Rydberg gases in the presence of decay with the rate $\gamma = 2\pi \times 1$ MHz. (a) Rydberg density, i.e., $(\sum_i \langle \sigma_z^{(i)} \rangle / N + 1) / 2$, obtained from a cluster size of 9×9 exhibits a discontinuity for different values of detuning Δ signaling a first-order transition, with the steplike discreteness being due to the numerical resolution. (b) The pair correlation function g_2 demonstrates a blocked region for low-density phase (solid lines) and a facilitated region for high-density phase (dotted lines). In all cases, the driving strength Ω was chosen right below the transition (solid) or right above it (dotted). (c) The steady-state phase diagram is obtained by finite-size scaling of the variational results which resembles a lattice liquid-gas transition.

in which correlations over a cluster of N sites are accounted for. Hence, we can easily detect the presence of dissipative phase transitions by observing nonanalytic behavior of steady state observables. Note that while our approach shares some similarities to previous approaches based on cluster mean-field theory [33,34], a variational treatment of product states and mean-field theory are not equivalent, in contrast to the equilibrium case. Therefore, the variational character of our approach allows us to avoid some pitfalls associated with mean-field theory in open systems [11,35,36].

A crucial aspect of our variational approach is to accurately describe the pair correlation function $g_2(r_{ij}) = \langle P_r^{(i)} P_r^{(j)} \rangle / \langle P_r^{(i)} \rangle \langle P_r^{(j)} \rangle$ with relatively few variational parameters that need to be optimized. From perturbation theory in the strongly blocked regime [37], one can expect that the pair correlation function behaves for small distances as $g_2(r_{ij}) \sim r_{ij}^6$, while for weak interactions at large distances, one would expect $\lim_{r_{ij} \rightarrow \infty} g_2(r_{ij}) = 1$. An expansion satisfying these two limits is given by

$$g_2(r) = \frac{\alpha_6 r^6}{\alpha_6 r^6 + \sum_{0 \leq k < 6} \alpha_k r^k}, \quad (6)$$

where the α_k are variational parameters. Here, we truncate the sum after the second order, for which we find that Eq. (6) is in good quantitative agreement with exact numerical simulations of small systems. For correlation functions involving σ_x or σ_y , we assume an exponential decay, with the only exception being the correlator $\langle \sigma_y^{(i)} \sigma_z^{(j)} \rangle - \langle \sigma_y^{(i)} \rangle \langle \sigma_z^{(j)} \rangle$, which is inherently linked to $g_2(r)$ through the Lindblad master equation [21].

Steady state phase diagram.—First, we focus on the case without any dephasing, i.e., $\gamma_p = 0$. Without any dissipation, the ground state phase diagram of Eq. (2) on a lattice for $\Delta > 0$ consists of a series of crystalline phases that can

be either commensurate or incommensurate with the underlying lattice, and a paramagnetic phase for sufficiently strong driving strength Ω [38–40]. Including dissipation, we find a vastly different phase diagram for the nonequilibrium steady state. Overall, we find the presence of two competing phases, see Fig. 2, one at low densities exhibiting the characteristic pair correlation function $g_2(r)$ of the Rydberg blockade, and one at higher densities in which the Rydberg atoms are either uncorrelated or even exhibiting bunching of neighboring Rydberg excitations, i.e., leading to a complete lifting of the Rydberg blockade. We note that the second phase also covers the so-called antiblockade or facilitated regime [41–43], where the detuning cancels the longitudinal field term arising from the interaction, resulting in an effectively purely transversal Ising model. Hence, we refer to the two phases as “blockade phase” and “facilitation phase,” respectively. We find that the two phases are separated by a first order transition that stretches throughout the entire parameter space. To determine the position of the first-order line in the limit of infinitely large clusters, we perform an analysis in close analogy to finite-size scaling, using cluster sizes of 5×5 , 7×7 , and 9×9 . The choice of odd numbers is twofold; first, it considerably simplifies the expressions for the variational norm as it can be constructed around a site at the center of the lattice. Second, even and odd sites have slightly different scaling behavior, so focusing on only one of them achieves faster convergence. The result of the cluster scaling analysis is shown in Fig. 2(c). Furthermore, even in the facilitation phase, we find that the density of Rydberg excitations is comparatively low close to the transition, which we attribute to the first excitation still being suppressed by the van der Waals interaction, which is much stronger than the driving strength Ω . Remarkably, in stark contrast to the ground state phase diagram, we find no evidence for additional crystalline phases that are commensurate with the underlying lattice, as the first order line

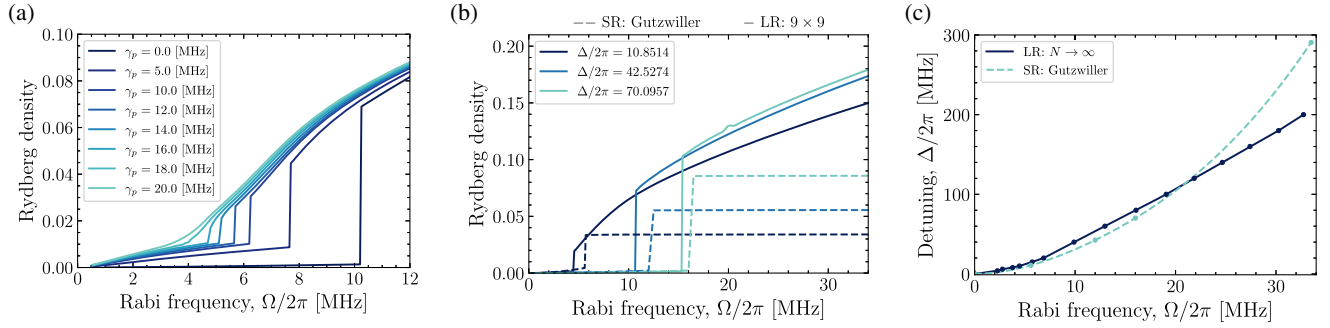


FIG. 3. Extensions to the basic model. (a) Inclusion of dephasing results in the termination of the first order line with a critical point. For $\Delta = 2\pi \times 40$ MHz, criticality appears at $\gamma_p = 2\pi \times 16$ MHz with the cluster size of 9×9 . (b) Variational results for an effective short-range interacting model using a Gutzwiller ansatz (dashed lines) in comparison with the long-range interacting model using the correlated ansatz (solid lines). (c) For relatively weak driving, the phase transition in dissipative Rydberg gases can be effectively described by a short-range interacting model.

appears to be a smooth function, with other quantities such as the blockade radius behaving in a similar way.

Dephasing-induced criticality.—Without dephasing, the numerical results are consistent with the first order line extending all the way to $\Delta = 0$, without triggering any critical behavior, in contrast to both the ground state phase diagram and the steady-state phase diagram for purely coherent evolution [23,44]. However, as already known from other dissipative models exhibiting first-order transitions [12,45,46], such first order lines between two competing phases can be turned critical by injecting additional dephasing noise into the dynamics. Within our variational approach, we also observe this behavior for the long-range interacting case, see Fig. 3(a). In particular, we find the critical point emerging for a detuning of $\Delta = 2\pi \times 40$ MHz at $\gamma_p = 2\pi \times 16$ MHz. Such a level dephasing can be realized experimentally by noise on the excitation laser, opening a very promising route to study dissipative criticality in such a setting.

Effective short range models.—As already mentioned, the inherent challenges with studying open quantum many-body systems has led to most theoretical works replacing the long-range interaction in dissipative Rydberg gases by a short-range interaction. While it is clear that this is inadequate to correctly describe the Rydberg blockade, one may ask whether such a simplification can still be used to describe dissipative Rydberg gases, especially since properly renormalized short-range models have had some success in describing experiments even in the blocked regime [12]. To this end, we develop a systematic way to derive effective short-range models [21]. Here, we consider the situation where the detuning is chosen in such a way that it realizes an antiblockade configuration at a particular distance r' . Then, we assume that all lattice sites in between are effectively frozen and consider an effective model involving only the remaining sites. As we operate in an antiblockade configuration, we obtain a purely transversal Ising model, i.e.,

$$H_{\text{eff}} = \frac{\hbar\Omega}{2} \sum_i \sigma_x^{(i)} + J_{\text{eff}}(r_d) \sum_{\langle ij \rangle} \sigma_z^{(i)} \sigma_z^{(j)}, \quad (7)$$

where $J_{\text{eff}}(r_d)$ denotes the strength of the nearest-neighbor Ising interaction which accounts for van der Waals interaction excluding terms from the nearest-neighbor up to a truncation distance $r_d < r'$ [21].

We can benchmark the validity of the effective short-range model by performing variational calculations. For the short-range model, we utilize a Gutzwiller ansatz, which has been shown to give reliable quantitative estimates of the position of the first order transition [16]. Figures 3(b) and 3(c) confirm that the short-range Ising model is in good quantitative agreement with the long-range interacting model after accounting for the number of excluded sites by rescaling the Rydberg density by a factor of $(r_d + 1)^2$, provided that the driving strength Ω is relatively small. For larger values of the driving strength, resulting in a decreasing truncation radius r_d , the correspondence becomes worse, although the position of the first order transition remains quite accurate over a substantially larger region. This is somewhat counterintuitive, as in the limit where the truncation distance vanishes, one would expect a short-range model to be valid, although there are cases when considering classical rate equations instead of a Lindblad master equation, where a van der Waals interaction is not decaying sufficiently fast to allow for a replacement by a nearest-neighbor interaction [47]. However, while the short-range model is able to determine the position of the first order transition, the properties of the competing phases are vastly different. In the short-range case, the low-density phase is a weakly correlated gas of Rydberg excitations, while the high-density phase behaves similar to an incompressible liquid. In contrast, the low-density phase in the blocked regime is strongly correlated, while positive correlations and compressibility persist in the high-density phase. Additionally, we find the steady state being unique except on the first order transition line. This is

consistent with the picture that there are no additional symmetries of the master equation away from the transition line [48].

In summary, we have analyzed the stationary properties of strongly interacting Rydberg gases under driving and dissipation using a variational treatment properly capturing long-range correlations. In stark contrast to the ground state phase diagram, the steady state of dissipative Rydberg gases features a single first-order phase transition between a blocked phase and a facilitation phase, without any commensurability effects from the underlying optical lattice. The first-order line can be tuned critical by incorporating additional dephasing noise, leading to a very promising route to investigate dissipative criticality in an open quantum system. Finally, we find that despite strong blockade effects, effective short-range descriptions of dissipative Rydberg gases can be successfully used to compute the phase boundaries of the steady state phase diagram and hence can serve as a minimal model, however, the interpretation of the individual phases requires taking the long-range correlations into account.

We thank C. Groß, P. Schauß, and J. Zeiher for valuable discussions on the experimental realization of dissipative Rydberg gases. This work was funded by the Volkswagen Foundation, by the Deutsche Forschungsgemeinschaft (DFG, German Research Foundation) within SFB 1227 (DQ-mat, project A04), SPP 1929 (GiRyd), and under Germany's Excellence Strategy–EXC-2123 QuantumFrontiers–90837967.

*javad.kazemi@itp.uni-hannover.de
†weimer@tu-berlin.de

- [1] C. G. Wade, M. Marcuzzi, E. Levi, J. M. Kondo, I. Lesanovsky, C. S. Adams, and K. J. Weatherill, Terahertz-driven phase transition applied as a room-temperature terahertz detector, *arXiv:1709.00262*.
- [2] S. Helmrich, A. Arias, G. Lothead, T. M. Wintermantel, M. Buchhold, S. Diehl, and S. Whitlock, Signatures of self-organized criticality in an ultracold atomic gas, *Nature (London)* **577**, 481 (2020).
- [3] H. Weimer, A. Kshetrimayum, and R. Orús, Simulation methods for open quantum many-body systems, *Rev. Mod. Phys.* **93**, 015008 (2021).
- [4] D. Jaksch, J. I. Cirac, P. Zoller, S. L. Rolston, R. Côté, and M. D. Lukin, Fast Quantum Gates for Neutral Atoms, *Phys. Rev. Lett.* **85**, 2208 (2000).
- [5] M. D. Lukin, M. Fleischhauer, R. Côté, L. M. Duan, D. Jaksch, J. I. Cirac, and P. Zoller, Dipole Blockade and Quantum Information Processing in Mesoscopic Atomic Ensembles, *Phys. Rev. Lett.* **87**, 037901 (2001).
- [6] K. Singer, M. Reetz-Lamour, T. Amthor, L. G. Marcassa, and M. Weidemüller, Suppression of Excitation and Spectral Broadening Induced by Interactions in a Cold Gas of Rydberg Atoms, *Phys. Rev. Lett.* **93**, 163001 (2004).
- [7] R. Heidemann, U. Raitzsch, V. Bendkowsky, B. Butscher, R. Löw, L. Santos, and T. Pfau, Evidence for Coherent Collective Rydberg Excitation in the Strong Blockade Regime, *Phys. Rev. Lett.* **99**, 163601 (2007).
- [8] P. Schauß, M. Cheneau, M. Endres, T. Fukuhara, S. Hild, A. Omran, T. Pohl, C. Gross, S. Kuhr, and I. Bloch, Observation of spatially ordered structures in a two-dimensional Rydberg gas, *Nature (London)* **491**, 87 (2012).
- [9] H. Bernien, S. Schwartz, A. Keesling, H. Levine, A. Omran, H. Pichler, S. Choi, A. S. Zibrov, M. Endres, M. Greiner *et al.*, Probing many-body dynamics on a 51-atom quantum simulator, *Nature (London)* **551**, 579 (2017).
- [10] T. E. Lee and M. C. Cross, Spatiotemporal dynamics of quantum jumps with Rydberg atoms, *Phys. Rev. A* **85**, 063822 (2012).
- [11] H. Weimer, Variational Principle for Steady States of Dissipative Quantum Many-Body Systems, *Phys. Rev. Lett.* **114**, 040402 (2015).
- [12] H. Weimer, Variational analysis of driven-dissipative Rydberg gases, *Phys. Rev. A* **91**, 063401 (2015).
- [13] A. Kshetrimayum, H. Weimer, and R. Orús, A simple tensor network algorithm for two-dimensional steady states, *Nat. Commun.* **8**, 1291 (2017).
- [14] J. Panas, M. Pasek, A. Dhar, T. Qin, A. Geißler, M. Hafez-Torbati, M. E. Sorantin, I. Titvinidze, and W. Hofstetter, Density-wave steady-state phase of dissipative ultracold fermions with nearest-neighbor interactions, *Phys. Rev. B* **99**, 115125 (2019).
- [15] V. P. Singh and H. Weimer, Driven-Dissipative Criticality within the Discrete Truncated Wigner Approximation, *Phys. Rev. Lett.* **128**, 200602 (2022).
- [16] J. Kazemi and H. Weimer, Genuine Bistability in Open Quantum Many-Body Systems, *arXiv:2111.05352*.
- [17] H.-P. Breuer and F. Petruccione, *The Theory of Open Quantum Systems* (Oxford University Press, Oxford, 2002).
- [18] F. Robicheaux and J. V. Hernández, Many-body wave function in a dipole blockade configuration, *Phys. Rev. A* **72**, 063403 (2005).
- [19] R. Löw, H. Weimer, J. Nipper, J. B. Balewski, B. Butscher, H. P. Büchler, and T. Pfau, An experimental and theoretical guide to strongly interacting Rydberg gases, *J. Phys. B* **45**, 113001 (2012).
- [20] C. Nill, K. Brandner, B. Olmos, F. Carollo, and I. Lesanovsky, Many-Body Radiative Decay in Strongly Interacting Rydberg Ensembles, *Phys. Rev. Lett.* **129**, 243202 (2022).
- [21] See Supplemental Material at <http://link.aps.org/supplemental/10.1103/PhysRevLett.130.163601> for a derivation of the effectively local jump operators, the details of the variational ansatz, and the derivation of the effective short-range model, which includes Refs. [16,20,22–31].
- [22] P. Navez and R. Schützhold, Emergence of coherence in the Mott-insulator–superfluid quench of the Bose-Hubbard model, *Phys. Rev. A* **82**, 063603 (2010).
- [23] H. Weimer, R. Löw, T. Pfau, and H. P. Büchler, Quantum Critical Behavior in Strongly Interacting Rydberg Gases, *Phys. Rev. Lett.* **101**, 250601 (2008).
- [24] F. Reiter and A. S. Sørensen, Effective operator formalism for open quantum systems, *Phys. Rev. A* **85**, 032111 (2012).
- [25] J. H. Gurian, P. Cheinet, P. Huillery, A. Fioretti, J. Zhao, P. L. Gould, D. Comparat, and P. Pillet, Observation of a

- Resonant Four-Body Interaction in Cold Cesium Rydberg Atoms, *Phys. Rev. Lett.* **108**, 023005 (2012).
- [26] V. M. Entin, E. A. Yakshina, D. B. Tretyakov, I. I. Beterov, and I. I. Ryabtsev, Spectroscopy of the three-photon laser excitation of cold Rubidium Rydberg atoms in a magneto-optical trap, *J. Exp. Theor. Phys.* **116**, 721 (2013).
- [27] D. Petrosyan, M. Hönig, and M. Fleischhauer, Spatial correlations of Rydberg excitations in optically driven atomic ensembles, *Phys. Rev. A* **87**, 053414 (2013).
- [28] P. Virtanen *et al.*, SciPy 1.0: Fundamental algorithms for scientific computing in PYTHON, *Nat. Methods* **17**, 261 (2020).
- [29] B. Sun and F. Robicheaux, Numerical study of two-body correlation in a 1D lattice with perfect blockade, *New J. Phys.* **10**, 045032 (2008).
- [30] B. Olmos, M. Müller, and I. Lesanovsky, Thermalization of a strongly interacting 1D Rydberg lattice gas, *New J. Phys.* **12**, 013024 (2010).
- [31] A. Actor, Evaluation of multidimensional linear zeta functions, *J. Number Theory* **35**, 62 (1990).
- [32] S. Weber, C. Tresp, H. Menke, A. Urvoy, O. Firstenberg, H. P. Büchler, and S. Hofferberth, Tutorial: Calculation of Rydberg interaction potentials, *J. Phys. B* **50**, 133001 (2017).
- [33] J. Jin, A. Biella, O. Viyuela, L. Mazza, J. Keeling, R. Fazio, and D. Rossini, Cluster Mean-Field Approach to the Steady-State Phase Diagram of Dissipative Spin Systems, *Phys. Rev. X* **6**, 031011 (2016).
- [34] J. Jin, A. Biella, O. Viyuela, C. Ciuti, R. Fazio, and D. Rossini, Phase diagram of the dissipative quantum Ising model on a square lattice, *Phys. Rev. B* **98**, 241108(R) (2018).
- [35] M. F. Maghrebi and A. V. Gorshkov, Nonequilibrium many-body steady states via Keldysh formalism, *Phys. Rev. B* **93**, 014307 (2016).
- [36] V. R. Overbeck, M. F. Maghrebi, A. V. Gorshkov, and H. Weimer, Multicritical behavior in dissipative Ising models, *Phys. Rev. A* **95**, 042133 (2017).
- [37] M. Müller, I. Lesanovsky, H. Weimer, H. P. Büchler, and P. Zoller, Mesoscopic Rydberg Gate Based on Electromagnetically Induced Transparency, *Phys. Rev. Lett.* **102**, 170502 (2009).
- [38] H. Weimer and H. P. Büchler, Two-Stage Melting in Systems of Strongly Interacting Rydberg Atoms, *Phys. Rev. Lett.* **105**, 230403 (2010).
- [39] B. Capogrosso-Sansone, C. Trefzger, M. Lewenstein, P. Zoller, and G. Pupillo, Quantum Phases of Cold Polar Molecules in 2D Optical Lattices, *Phys. Rev. Lett.* **104**, 125301 (2010).
- [40] E. Sela, M. Punk, and M. Garst, Dislocation-mediated melting of one-dimensional Rydberg crystals, *Phys. Rev. B* **84**, 085434 (2011).
- [41] C. Ates, T. Pohl, T. Pattard, and J. M. Rost, Many-body theory of excitation dynamics in an ultracold Rydberg gas, *Phys. Rev. A* **76**, 013413 (2007).
- [42] A. Urvoy, F. Ripka, I. Lesanovsky, D. Booth, J. P. Shaffer, T. Pfau, and R. Löw, Strongly Correlated Growth of Rydberg Aggregates in a Vapor Cell, *Phys. Rev. Lett.* **114**, 203002 (2015).
- [43] M. M. Valado, C. Simonelli, M. D. Hoogerland, I. Lesanovsky, J. P. Garrahan, E. Arimondo, D. Ciampini, and O. Morsch, Experimental observation of controllable kinetic constraints in a cold atomic gas, *Phys. Rev. A* **93**, 040701(R) (2016).
- [44] R. Löw, H. Weimer, U. Krohn, R. Heidemann, V. Bendkowsky, B. Butscher, H. P. Büchler, and T. Pfau, Universal scaling in a strongly interacting Rydberg gas, *Phys. Rev. A* **80**, 033422 (2009).
- [45] M. Marcuzzi, E. Levi, S. Diehl, J. P. Garrahan, and I. Lesanovsky, Universal Nonequilibrium Properties of Dissipative Rydberg Gases, *Phys. Rev. Lett.* **113**, 210401 (2014).
- [46] M. Raghunandan, J. Wrachtrup, and H. Weimer, High-Density Quantum Sensing with Dissipative First Order Transitions, *Phys. Rev. Lett.* **120**, 150501 (2018).
- [47] M. Hoening, W. Abdussalam, M. Fleischhauer, and T. Pohl, Antiferromagnetic long-range order in dissipative Rydberg lattices, *Phys. Rev. A* **90**, 021603(R) (2014).
- [48] V. V. Albert and L. Jiang, Symmetries and conserved quantities in Lindblad master equations, *Phys. Rev. A* **89**, 022118 (2014).